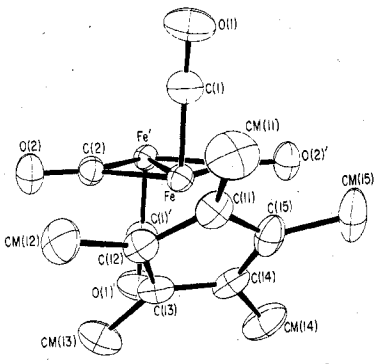


**Figure 2.** The $(\eta^5\text{-}C_5C_5)Fe_2(CO)_4$ fragment of $[(\eta^5\text{-}C_5Me_5)Fe(CO)_2]_2$ as viewed along the Fe–Fe bond. Note that the Fe–C(1) and C(11)–Ω (Ω = Cp ring centroid) vectors are eclipsed (dihedral angle = 4.2°). The ellipsoids of thermal motion are scaled to enclose 50% probability.

As in other Mp complexes one hydrogen atom of each methyl group is exo to the metal atom.[14]

The orientations of the cyclopentadienyl rings are very similar in the two complexes. The centroids of the $C_5$ rings, the iron atoms, and the terminal carbonyl carbon atoms are planar, and the angle between this plane and the $C_5$ plane of the Mp group is 91.4 (2)° in $[MpFe(CO)_2]_2$. One important difference between the two structures is that in the title compound the terminal carbonyl ligand is eclipsed with respect to C(11) (the C(11)–Ω–Fe–CO dihedral angle is 4.6 (2)°) rather than staggered (see Figure 2). There is an approximate mirror plane through C(11), the midpoint of C(13)–C(14), and the metal atom just as is observed in $[CpFe(CO)_2]_2$. In the above-mentioned low-temperature study[12] of the unsubstituted dimer a variation in bond lengths in the cyclopentadienyl fragment was attributed to the dominance of the $e^+$ molecular orbital (antisymmetric with respect to the mirror plane) because the observed variations were consistent with the symmetry of this molecular orbital. This pattern of bond lengths in the Cp fragment is consistent with a "diolefin" ring geometry. In the permethylated dimer the presence of the methyl groups, and likely differences in stuctural packing effects, has apparently reduced the thermal motion of the ring carbon atoms. The result is much the same as if the temperature were lowered, thus enabling us to examine small variations in C(ring)–C(ring) bond lengths.[15] (In this case $3\sigma$ = 0.013 Å for a C(ring)–C(ring) bond comparisons.) We do not observe any such variation, however. The range of C–C distances within the ring is quite small (1.422 (3)–1.431 (3) Å), and even the small fluctuations present do not reflect the symmetry of the molecular mirror plane and hence are not consistent with dominance of the $e^+$ (or $e^-$) molecular orbital. We therefore conclude that if the fluctuations noted in the structure of $[CpFe(CO)_2]_2$ do indeed stem from electronic effects, the presence of methyl groups in the titular complex has altered these effects. It is equally probable, however, that the methyl groups have effectively "masked" the fivefold symmetry of the $C_5$ ring and have mainly altered the packing forces within the lattice.[16]

The issue of distortions in cyclopentadienyl ligands remains an open question. While it is unquestionably true that electron localization within the π-network can cause distortions, the magnitude and observability of these distortions remains unknown.[17] It may be that the energies associated with these distortions are small compared to packing forces or other subtle electronic effects.

**Acknowledgment.** We wish to thank H. M. Feder and J. W. Rathke of the Argonne Chemical Engineering Division for helpful discussions and D. Slocum, J. Bencini, and S. Diviaj of Southern Illinois University, Carbondale, IL, for supplying the compound.

**Registry No.** $[MpFe(CO)_2]_2$, 12132-03-5.

**Supplementary Material Available:** A listing of observed and calculated structure factor amplitudes (7 pages). Ordering information is given on any current masthead page.

(16) It was suggested by one reviewer that the eclipsed orientation of the terminal Fe–CO with respect to the Mp ring has removed any preference toward the $e^+$, or $e^-$, molecular orbital.
(17) Wheatley, P. J. In "Perspectives in Structural Chemistry"; Dunitz, J. D., Ibers, J. A., Eds.; Wiley: New York, 1967; Vol. 1, p 1.

Contribution from the Laboratoire de Physicochimie Minérale, Université Paris Sud, 91405 Orsay Cedex, France, Laboratoire de Spectrochimie Infrarouge et Raman, CNRS-2, 94320 Thiais, France, and Laboratoire de Chimie Physique, Université Paris Nord, 93410 Villetaneuse, France

# Vibrational Study of Layered $MPX_3$ Compounds and of Some Intercalates with $Co(\eta^5\text{-}C_5H_5)_2^+$ or $Cr(\eta^6\text{-}C_6H_6)_2^+$

Y. MATHEY, R. CLEMENT, C. SOURISSEAU,* and G. LUCAZEAU

*Received November 28, 1979*

Raman (10–800 $cm^{-1}$) and IR (10–4000 $cm^{-1}$) spectra of layered compounds represented by the general formula $MPX_3$ where M = Mn, Cd, or Zn and X = S or Se have been recorded in the 300–10 K temperature range. $MnPS_3$ and $CdPS_3$ compounds intercalated with $Co(\eta^5\text{-}C_5H_5)_2^+$ and $Cr(\eta^6\text{-}C_6H_6)_2^+$ cations, corresponding to formula $MPS_3{\cdot}0.33(\pi\text{-}R)_2\mathcal{M}$, were investigated under the same conditions. Host lattice vibrations give rise to a pattern characteristic of the $PS_3$ entity and are not strongly perturbed by intercalated molecules. New low-frequency bands observed for the Mn compounds can be interpreted in terms of a different unit cell multiplicity. Guest ion frequencies are practically the same as those of their iodide salts, which indicates weak interactions between cations and host lattices. Finally, polarized infrared spectra of platelets show that $(\pi\text{-}R)_2\mathcal{M}^+$ ion rings are oriented perpendicular to (00*l*) host lattice layer planes.

## Introduction

This work has been undertaken as a part of a general vibrational study of layered compounds able to intercalate guest molecules or ions. It has been shown for different superionic conductors of the β-alumina type that infrared and Raman spectroscopies yield a wealth of information concerning structures and dynamics of guest ions such as $H_3O^+$, $NH_4^+$, $Na^+$, $Ag^+$, ....[1-3] Most of the compounds represented by the

* To whom correspondence should be addressed at the Laboratoire de Spectrochimie Infrarouge et Raman.

(1) Ph. Colomban, J. P. Boilot, A. Kahn, and G. Lucazeau, *Nouv. J. Chim.*, **2**, 21 (1978).

0020-1669/80/1319-2773$01.00/0 

general formula $MPS_3$ belong to the $MS_2$ structural family and are broad-band semiconductors. Some of them function as cathodes in lithium batteries where electron transfer of an electrochemical reaction occurs via intercalation of the material following the scheme: $MPS_3 + xLi^+ + xe^- \rightarrow Li_xMPS_3$.[4] Preliminary vibrational studies of some $Li_xMPS_3$ compounds have shown that Raman spectra of host lattices were not modified by intercalation.[5] It appeared interesting to inquire about the effect of large cations such as $Co(\eta^5\text{-}C_5H_5)_2^+$ and $Cr(\eta^6\text{-}C_6H_6)_2^+$ (noted hereafter as $CoCp_2^+$ and $CrBz_2^+$, respectively) which can be intercalated in $CdPS_3$ and $MnPS_3$ and lead to definite compounds of general formula $MPS_3 \cdot 0.33(\pi\text{-}R)_2\mathcal{M}$.[6]

We have investigated infrared and Raman spectra of these compounds in order to (i) check the oxidation state of the guest species, (ii) determine the orientation of ions with respect to the host lattice, (iii) find out whether the electron transfer affects the host lattice, and (iv) see if the rotational jumps of rings, responsible for the disordered crystalline phases of $CoCp_2$ and $CrBz_2$ at room temperature,[7] do persist when these molecules are intercalated in $MPS_3$.

## Experimental Section

**1. Samples.** Pure $MPS_3$ phases (M = Mn, Cd, Zn) were synthesized by heating the metal or its sulfide (CdS, ZnS) with a stoichiometric amount of sulfur and red phosphorus according to the procedure described in ref 8. They were characterized by chemical analysis of the elements and by powder X-ray diffraction. The $MnPSe_3$ compound was obtained from Rouxel.[4]

Intercalates of these phases with dicyclopentadienylcobalt and bis(benzene)chromium were synthesized according to the methods described in ref 6 and 9: intercalates obtained at room temperature from aqueous solutions of cobaltocenium or bis(benzene)chromium iodides were more suitable for Raman studies than those synthesized at 120 °C following ref 9. Moreover, we found that a single crystal of $MnPS_3$, treated with an aqueous solution of $CoCp_2I$ for about 4 days, led to a monocrystalline intercalate. Intercalation of $CdPS_3$ was performed by addition of a reducing agent such as sodium dithionite in aqueous solutions of iodide salts. It should be pointed out that intercalates obtained by "wet" methods contain a small amount (2–3%) of water as observed by infrared spectroscopy.

**2. Spectra.** Raman spectra were obtained with a Coderg T 800 instrument equipped with a krypton laser (6471 Å) and with an ionized argon laser (4880 and 5145 Å). At room temperature, $MnPS_3$ was studied as a single crystal but because of the thinness ($\sim$30 $\mu$m) of the sample only a weak polarization effect was observed. Changes in the relative intensity of the 245- and 275-$cm^{-1}$ bands were observed for different scattering geometries.

Infrared spectra were recorded on Perkin-Elmer 180 and Polytec FIR 30 spectrometers in the 4000–200- and 300–10-$cm^{-1}$ ranges, respectively. Monocrystalline platelets 3 × 3 × 0.03 mm were studied by using a beam condenser; polycrystalline samples were dispersed in Nujol and Fluorolube.

## Structure and Symmetry Considerations

**1. $MPX_3$ Unintercalated Compounds.** The structure of the $MPS_3$ lamellar compounds is only known for $FePS_3$ and $FePSe_3$:[10] it derives from $CdI_2$ structure and can be described

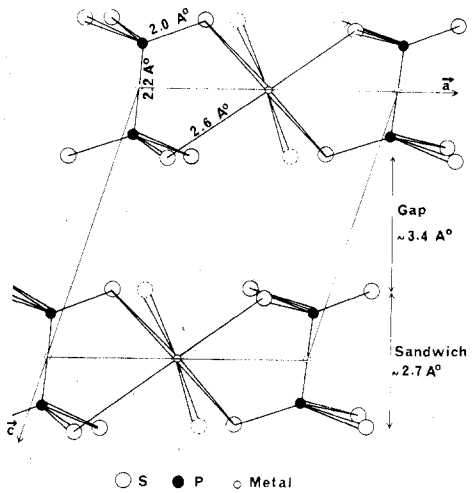


**Figure 1.** Perspective view of monoclinic $MPS_3$ structure ($C2/m$). (Atoms in unbroken lines have $y$ values between $+^1/_6$ and $-^1/_6$ and those in broken lines are at $y = \pm^1/_3$.)

(Figure 1) as a succession of sandwiches composed of two layers of sulfur (or selenium) atoms between which are located metals and pairs of phosphorus atoms. The sandwiches are weakly bonded together, and the intersandwich gap will be filled with cations after intercalation. All the layers are stacked along the $\vec{a}\wedge\vec{b}$ axis (exactly along the $\vec{c}$ axis for the selenium derivative).

For $FePS_3$, the sulfur atoms are arranged approximately following a cubic packing and the crystal structure is described by the $C2/m$ ($C_{2h}^3$) space group, while for $FePSe_3$ the selenium atoms form a hexagonal network and the structure is described by $R3$ ($C_3^4$) space group. In both compounds three kinds of chemical units can be recognized (Figure 1):

(i) Each metal ion is surrounded by six sulfur or selenium atoms defining a pseudooctahedron (the mean Fe–S distance is equal to 2.6 Å).

(ii) Each phosphorus atom is bonded to three chalcogen atoms, the mean P–S distance being equal to 2.0 Å as in similar compounds.[11] $PS_3$ groups define flat pyramids (P atoms are $\sim$0.5 Å out of $S_3$ planes) and in the first approximation can be described by $D_{3h}$ symmetry.

(iii) Each $PX_3$ group is connected with another group (through a center of inversion in the sulfide compound), giving rise to a $P_2X_6$ entity, the P–P distance being equal to $\sim$2.2 Å: the symmetry of the $P_2X_6$ species is close to that of $D_{3d}$ point group. $MnPS_3$, $ZnPS_3$, and $CdPS_3$ structures belong to the same monoclinic system.[12] Mn and Zn compounds have nearly the same lattice parameters as $FePS_3$, and one can assume the previous considerations valid for these compounds. $MnPSe_3$ as $FePSe_3$ belongs to the hexagonal system, and, such a structure being noncentrosymmetric, $PSe_3$ units are no longer related by a center of inversion.

**2. Intercalated Compounds.** There are no accurate structural data for intercalated compounds. X-ray powder diagrams[6] have shown that interlayer distances increase with intercalation, 5.76 Å for $CrBz_2$ and 5.32 Å for $CoCp_2$. No superstructure has been evidenced among the (00$l$) lines.

For some $MS_2$-layered transition-metal compounds intercalated with $CoCp_2$, Dines[13] has connected the "$c$" lattice parameter expansion with the dimensions of the organometallic

(2) Ph. Colomban, A. Mercier, G. Lucazeau, and A. Novak, *J. Chem. Phys.*, **67**, 5244 (1977).
(3) Ph. Colomban and G. Lucazeau, *J. Chem. Phys.*, **72**, 1213 (1980).
(4) R. Brec, D. M. Schleich, G. Ouvrard, A. Louisy, and J. Rouxel, *Inorg. Chem.*, **18**, 1814 (1979), and references therein.
(5) G. Lucazeau, unpublished results.
(6) R. Clement and M. L. H. Green, *J. Chem. Soc., Dalton Trans.*, **10**, 1566 (1979).
(7) K. Chor, C. Sourisseau, and G. Lucazeau, *Proc. Int. Conf. Raman Spectrosc., 6th*, **2**, 432 (1978).
(8) W. Klingen, R. Ott, and H. Hahn, *Z. Anorg. Allg. Chem.*, **396**, 271 (1973).
(9) J. P. Audiere, R. Clement, Y. Mathey, and C. Mazieres, *Physica B+C (Amsterdam)*, **99B+C**, 133 (1980).
(10) W. Klingen, G. Eulenberger, and H. Hahn, *Z. Anorg. Allg. Chem.*, **401**, 97 (1973).
(11) M. Bouchetiere, P. Toffoli, P. Khodadad, and N. Rodier, *Acta Crystallogr. Sect. B*, **B34**, 384 (1978).
(12) F. Levy in "Physics and Chemistry of Materials with Layered Structures", Vol. 5, D. Reidel Publishing Co., Boston, 1976, p 217.
(13) M. B. Dines, *Science (Washington, D.C.)*, **188**, 1210 (1975).

Table I. Correlation Diagrams and Selection Rules in $MPX_3$ Compounds (X = S or Se)[a]

| approx type of motions | $PX_3$ $C_{3v}$ | $P_2X_6$ $D_{3d}$ | $PX_3$ $D_{3h}$ | factor groups[b] X = S $C_{2h}(Z = 2)$ | factor groups[b] X = Se $C_3(Z = 1)$ |
|---|---|---|---|---|---|
| $\nu_s(PX_3)$ | $A_1$ | $A_{1g} + A_{2u}$ | $A'_1$ | $A_g(R) + B_u(IR)$ | A(*R*, IR) |
| $\nu_d(PX_3)$ | E | $E_g + E_u$ | E′ | $\{A_g + B_g\}(R) + \{A_u + B_u\}(IR)$ | E(*R*, *IR*) |
| $\delta_s(PX_3)$ | $A_1$ | $A_{1g} + A_{2u}$ | $A''_2$ | $A_g(R) + B_u(IR)$ | A(R, *IR*) |
| $\delta_d(PX_3)$ | E | $E_g + E_u$ | E″ | $\{A_g + B_g\}(R) + \{A_u + B_u\}(IR)$ | E(*R*, IR) |
| $R'_z(PX_3)$ | $A_2$ | $A_{2g} + A_{1u}$ | $A'_2$ | $B_g(R) + A_u(IR)$ | A(R, IR) |
| $R'_{xy}(PX_3)$ | E | $E_g + E_u$ | E″ | $\{A_g + B_g\}(R) + \{A_u + B_u\}(IR)$ | E(*R*, IR) |
| $T'_z(PX_3)$ | $A_1$ | $A_{1g} + A_{2u}$ | $A''_2$ | $A_g(R) + B_u(IR)$ | A(R, *IR*) |
| $T'_{xy}(PX_3)$ | E | $E_g + E_u$ | E′ | $\{A_g + B_g\}(R) + \{A_u + B_u\}(IR)$ | E(*R*, *IR*) |
| $T'(M)$ | | | | $\{A_g + 2\ B_g\}(R) + \{A_u + 2\ B_u\}(IR)$ | A(R, IR) + E(R, IR) |

[a] (*R*) and (*IR*) mean strongly Raman- and infrared-active modes in the oriented-gas-model approximation when planar $PX_3$ groups are considered. [b] Acoustic modes have $A_u + 2\ B_u$ or A + E symmetries in $C_{2h}$ or $C_3$ factor groups, respectively.

cation and concluded that the principal axis of the guest ion lies parallel to the layers. Recently, this argument has been criticized,[14] the cation having roughly equal dimensions in three directions (6.6–6.8 Å). Thus, the structural problem of the guest orientation is still open.

## Selection Rules

There are two $MPS_3$ formulas per primitive cell for the sulfide compounds. All internal and lattice vibrations [30] can be classified under the $C_{2h}$ factor group according to $\Gamma = 8\ A_g + 7\ B_g + 6\ A_u + 9\ B_u$, and, since acoustic modes ($A_u + 2\ B_u$) must be subtracted, 15 Raman and 12 infrared bands are expected.

For $MnPSe_3$, there is one formula per unit cell and the crystalline vibrational modes are distributed following the 4 A + 4 E symmetry representations of the $C_3$ factor group plus three acoustic modes (A + E). All the vibrations are infrared and Raman active, and TO – LO splittings are expected for strong polar modes.

It is useful to consider the highest possible symmetries $C_{3v}$ and $D_{3h}$ of the $PX_3$ entities which give rise to a characteristic spectral pattern. However, the actual sites of phosphorus atoms are $C_2$ and $C_3$ for $MPS_3$ and $MPSe_3$, respectively. Table I gives the correlation diagrams between $C_{3v}$ and $D_{3h}$ "molecular" symmetries (plus $D_{3d}$ for $P_2X_6$ units) and $C_{2h}$ and $C_3$ factor group symmetries; translational motions of the metal ($T'(M)$) are also considered in both factor groups. If the site effect is weak, no splitting of degenerate modes is expected. Moreover, with the assumption of the oriented gas model, a normal mode which is, for instance, only Raman active in $D_{3h}$ will give rise to a strong Raman crystalline mode (underlined in Table I) and to a weak infrared counterpart: one expects thus eight Raman and four infrared strong bands for sulfide derivatives and seven Raman plus four infrared bands for the selenide compound. However, it is difficult to ascertain the number of expected strong infrared bands since the unit cell translations cannot be readily identified with translations of metal ions, their mass being smaller than or of the same order of magnitude as that of the $PS_3$ groups.

The chemical composition of intercalated compounds $MPS_3 \cdot 0.33(\pi\text{-}R)_2\mathcal{M}$ suggests that the primitive unit cell can have at least a threefold multiplicity. With the assumption of the same $C_{2h}$ factor group, the number of expected modes is thus 3 times bigger. In particular, acoustic modes could be observed as a result of Brillouin zone folding.

## Results and Discussion

**1. Unintercalated Compounds.** Infrared and Raman spectra of $MPX_3$ compounds are shown on Figure 2 in the 700–10-$cm^{-1}$ range where all the fundamentals are expected. Raman spectra, recorded at 10 K, of $ZnPS_3$ and $MnPS_3$ are also presented in Figure 2 because the quality of these spectra is much better at low temperature. The band wavenumbers and proposed assignments are reported in Table II. Finally, Figure

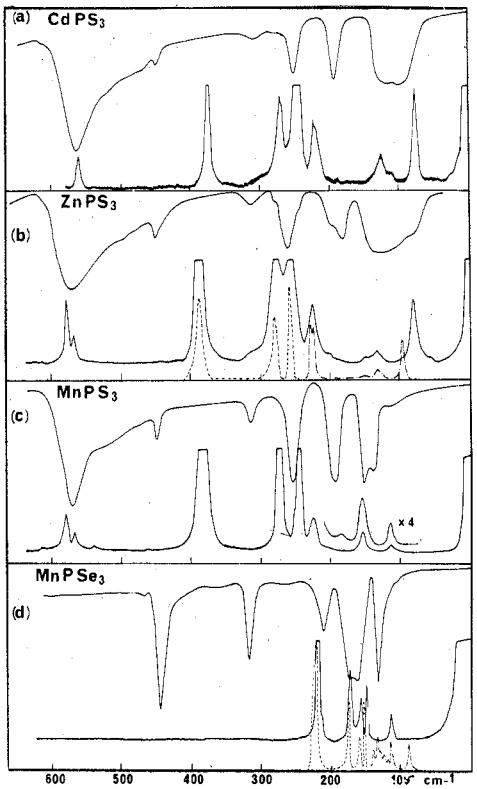


**Figure 2.** Infrared and Raman spectra (650–10 $cm^{-1}$) of $CdPS_3$ (a), $ZnPS_3$ (b), $MnPS_3$ (c), and $MnPSe_3$ (d) compounds: unbroken lines, room temperature spectra; broken lines, Raman spectra at 10 K for different intensity expansions.

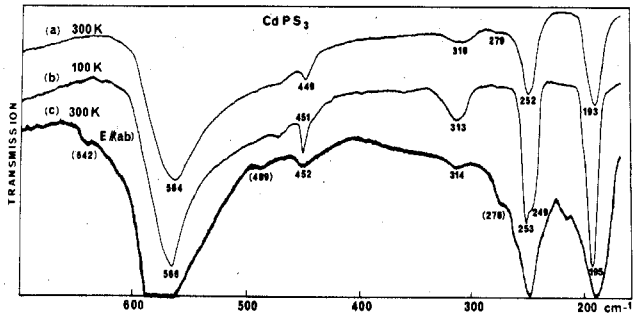


**Figure 3.** Infrared spectra (700–180 $cm^{-1}$) of a polycrystalline sample at 300 K (a) and 100 K (b) and of a monocrystalline platelet at 300 K (c) of the $CdPS_3$ compound.

(14) R. Clement, W. Davies, K. Ford, M. L. H. Green, and A. J. Jacobson, *Inorg. Chem.*, **17**, 2754 (1978).

**Table II.** Infrared and Raman Band Wavenumbers ($cm^{-1}$) of Some $MPX_3$ Compounds in the Solid State at 300 K[a]

| $CdPS_3$ | | $ZnPS_3$ | | $MnPS_3$ | | $MnPSe_3$ | | $\rho$[b] | | approx type of motions |
|---|---|---|---|---|---|---|---|---|---|---|
| IR | R | IR | R | IR | R | IR | R (10 K)[c] | $\nu$-($MnPS_3$)/$\nu$-($MnPSe_3$) | $\nu$-($MnPS_3$)/$\nu$-($CdPS_3$) | |
| 564 vs | 562 m | 571 vs | 577 m<br>568 w | 572 vs | 579 m<br>566 w | 468 vw<br>444 vs | | 1.29 | ~1.0 | $\nu_d(PX_3)$ |
| | | 510 w | 525 vw | 530 w | 539 w | 360 vw | | | | comb. |
| 449 m | | 451 m | | 450 m | | 316 m | | 1.42 | ~1.0 | $T'_z(PX_3)$ ($\nu$(P-P)) |
| | 376 vs | | 387 vs | | 378 vs | | 222 vs | 1.70 | ~1.0 | $\nu_s(PX_3)$ |
| 310 m | 298 vw | 312 m | 310 vw | 316 m | | 211 s | | 1.50 | ~1.0 | $\delta_s(PX_3)$ |
| 279 vw | 271 s | 274 vw | 277 vs | | 273 vs | | 173 s | 1.58 | ~1.0 | $\delta_d(PX_3)$ |
| 252 s | 248 vs | 259 s | 257 vs | 255 s | 244 vs | 171 s | | 1.49 | ~1.0 | $T'_{xy}(PX_3)$ |
| | 220 m | | 225 m | | 225 m | | 150 s | 1.50 | ~1.0 | $R'_{xy}(PX_3)$ |
| 193 s | 185 vw | 199 sh<br>182 s | 200 vw | 194 s | 185 vw | 162 s | 156 w | 1.20 | ~1.0 | $T'_{xy}(PX_3)$ |
| 120 s | 125 m | 140 s | 150 vw | 152 s | 154 m | 132 s | 133 w | ~1.16 | 1.25 | $R'_{xy}(PX_3)$? |
| 100 s | 110 w | 120 s | 130 w | 138 s | | (132 s) | 129 w | 1.05 | 1.38 | $T'(M)$ |
| | | 75 w | | 115 vw | 115 w | 105 vw | 120 vw | 1.10 | ? | $R'_z(PX_3)$? |
| | 77 s | | 79 m | | 110 w | | 112 w | 1.0 | 1.49 | $T'(M)$ |
| | 48 vw | | 55 vw | | | | 84 w | | | |

[a] Intensities of infrared (IR) and Raman (R) bands: vs, very strong; s, strong; m, medium; w, weak; vw, very weak; sh, shoulder. [b] Values of theoretical ratios ($\rho$) are equal to $(m(Se)/m(S))^{1/2} = 1.57$ and $(m(Cd)/m(Mn))^{1/2} = 1.43$, respectively. [c] For $MnPSe_3$, Raman frequencies at 10 K are reported because the quality of the spectrum has been greatly improved at low temperature.

3 shows infrared spectra (700–180 $cm^{-1}$) of a polycrystalline sample and of a platelet of $CdPS_3$.

**(a) Methods of Band Assignment.** First of all, the comparison of Raman and infrared spectra shows that most of the Raman bands do not coincide with an infrared one (Table I) for selenium as well as for sulfur compounds. In the former case this mutual exclusion indicates that the noncentrosymmetric $C_3$ factor group is not conclusive as far as the selection rules are concerned. Moreover, $C_{2h}$ factor group analysis predicts many more active modes than observed.

Since the band wavenumbers are very sensitive to the substitution of sulfur by selenium in the frequency range 700–180 $cm^{-1}$, the corresponding modes will be described essentially in terms of sulfur (selenium) motions. Moreover, in this range, the infrared bands, the relative intensity of which decreases drastically from powder to platelet transmission spectra (Figure 3), will be assigned with confidence to out-of-plane layer modes. In the low-frequency region (200–10 $cm^{-1}$), several bands are metal sensitive and shift when we go from $MnPS_3$ to $CdPS_3$: they correspond probably to translational motions of metal ions.

Finally, these spectra are very similar to those obtained for $Na_4P_2S_6{\cdot}6H_2O$[15] in which the existence of $P_2S_6^{4-}$ anions has been assumed. Under these conditions it should be tempting to describe our spectra in terms of internal modes of $P_2S_6$ entities and of translational motions of metals. However, such a model is not in agreement with new experimental data from polycrystalline and solution Raman spectra.[16] In particular, depolarization ratio measurements show that bands at 553 and 577 $cm^{-1}$, previously assigned to $\nu_s$ and $\nu_d$ ($PS_3$) modes by Bürger and Falius,[15] are both depolarized while only one band at 377 $cm^{-1}$ is polarized. Therefore, no Raman signal can be ascribed to a $\nu$(P–P) mode and the P–P interaction is not dominant. It seems more realistic to describe the spectra in terms of internal modes of $PS_3$ groups and by combining their in-phase and out-of-phase translational and rotational motions. For instance, one must keep in mind that the out-of-phase $T'_z$ $PS_3$ mode, corresponding to the $\nu$(P–P) vibration, is expected to give rise only to an infrared-active band (Table I).

**(b) Assignment of Group Vibrations and Approximate Types of Motions.** The strong infrared bands at about 570 $cm^{-1}$ are readily assigned to the $PS_3$ degenerate stretching mode. The occurrence of weak Raman bands at nearly the same frequencies shows that the coupling between two $PS_3$ units by correlation effect is very small. Furthermore, the broadness of infrared bands as well as the observation of two Raman components separated by about 10 $cm^{-1}$ is due to a small degeneracy removing: we can conclude that only a weak site effect is operative on $PS_3$ groups and that the oriented-gas-model approximation is justified. This mode shifts to 444 $cm^{-1}$ with substitution of sulfur by selenium, and the frequency ratio equal to 1.29 is smaller than the theoretical value, 1.57: as it is expected, a participation of phosphorus atom in this antisymmetric motion cannot be neglected (Table II).

The medium infrared band at 450 $cm^{-1}$ nearly disappears in the transmission spectrum of platelets (Figure 3). It corresponds to an out-of-plane vibration and may be assigned to the $\nu$(P–P) mode since the characteristic stretching frequency range for the P–P interactions of similar interatomic distances is about 400–600 $cm^{-1}$.[17] We have also localized this mode at 443 $cm^{-1}$ on the infrared spectrum of $Na_4P_2S_6{\cdot}6H_2O$.[16]

The next very strong Raman band at about 380 $cm^{-1}$ for the $MnPS_3$ compound shifts to 222 $cm^{-1}$ for $MnPSe_3$ and is assigned to the symmetric stretching mode of the $PS_3$ unit: the large frequency ratio, equal to 1.70, indicates that chalcogen atoms are mainly involved in this motion, but contributions of vibrational coupling cannot be excluded.

The assignments are not straightforward in the 320–150-$cm^{-1}$ frequency range, but the small number of observed intense bands is consistent with the above-mentioned weak crystal effects:

(i) First of all, the medium infrared band at about 315 $cm^{-1}$, which nearly disappears in the transmission spectra of platelets (Figure 3), is assigned with confidence to the symmetric $PS_3$ bending mode. Then, the strong Raman band at about 275 $cm^{-1}$ is ascribed to the degenerate $PS_3$ bending motion. It must be pointed out that the activity of these vibrations fits properly the oriented-gas-model predictions.

(ii) For the next four Raman bands in the range 250–150 $cm^{-1}$ we observe only three infrared counterparts; these bands, being strongly sulfur sensitive, are assigned to translational, $T'_{xy}$, and to rotational, $R'_{xy}$, motions of $PS_3$ units (Table II).

(15) H. Bürger and H. Falius, *Z. Anorg. Allg. Chem.*, **363**, 24 (1968).
(16) C. Sourisseau, Y. Mathey, and G. Lucazeau, unpublished results.
(17) K. Nakamoto in "Infrared and Raman Spectra of Inorganic and Coordination Compounds", Wiley, New York, 1978.

**Table III.** Infrared and Raman Band Wavenumbers ($cm^{-1}$) of $MnPS_3$ and $CdPS_3$ Compounds Intercalated with $CoCp_2^+$ in the Solid State at 300 K[a]

| $MnPS_3 \cdot 0.33CoCp_2^+$ | | $CdPS_3 \cdot 0.33CoCp_2^+$ | | approx type of motions |
|---|---|---|---|---|
| IR[b] | R | IR[b] | R | |
| 620 sh | 624 vw | 607 sh | 610 w | |
| 607 vs | | 596 vs | | |
| 590 sh | | 585 sh | | $\nu_d(PS_3)$ |
| 570 sh | 574 w | 565 sh | 562 w | |
| 556 vs | 560 | 553 vs | 556 sh | |
| 498 m | | 500 w | | $tilt_d(CoCp_2^+)$ |
| 459 s | | 460 m | | $\nu_a(CoCp_2)^+$ |
| 450 s | | 449 m | | $T'_z(PX_3)$ ($\nu$(P–P)) |
| 380 w | 386 vs | 375 w | 379 vs | $\nu_s(PS_3)$ (+$tilt_s(CoCp_2^+)$) |
| 321 s | | 313 s | | $\delta_s(PS_3)$ |
| 297 w | | 301 sh | | |
| | 319 s | | 316 s | $\nu_s(CoCp_2^+)$ |
| | 274 vs | | 273 s | $\delta_d(PS_3)$ |
| 266 m | | 252 s | | $T'_{xy}(PS_3)$ |
| 249 s | 245 w | 244 sh | 239 m | |
| 223 w | 224 vw | 222 w | 221 w | $R'_{xy}$ |
| 194 s | | 188 s | | $T'_{xy}(PS_3)$ |
| 174 sh | | 174 sh | | $\delta(CoCp_2^+)$ |
| 152 s | 154 vw | 120 s | 132 w | $R'_{xy}(PS_3) + T'(M)$ |
| 137 m | | 95 s | | |
| | 68 w | | | $R'$(Cp rings)[c] |
| 110 s | 109 vw | | | |
| 80 m | | | | |
| 70 sh | | 45 vw? | 49 w? | corner Brillouin zone lattice modes[c] |
| 22 s | | | | |

[a] Intensities as in Table II. [b] Infrared bands assigned to internal vibrations of Cp rings have also been observed: 3102 sh, 3093 m ($\nu$(CH)); 1411 s, 1340 vw, 1112 w ($\nu$(C-C)); 1006 m ($\delta$(CH)); 893 w, 860 s ($\gamma$(C-C)). [c] See explanation in the text.

However we note that the lowest frequency band is also metal sensitive and that its infrared activity is in disagreement with the oriented-gas-model prediction: this mode must be coupled with translations of metal ions.

(iii) Finally, the remaining low-frequency infrared and Raman bands (at 138 and 110 $cm^{-1}$ for $MnPS_3$) are essentially metal sensitive. They correspond to translational motion of metals ($T'$(M)) while a very weak band at about 115 $cm^{-1}$ can be tentatively assigned to the $R'_z$ $PS_3$ librations.

**(c) Force Constants in $PX_3$ Groups and P–P Interactions.** A valence force field has been calculated by application of usual formulas[18] with the assumption of "isolated" $P_2X_6$ units of $D_{3d}$ symmetry. From the principal force constants of $A_{1g}$, $A_{2u}$, $E_g$, and $E_u$ blocks, the stretching force constants $f_{P-P}$, $f_{P-S}$, and $f_{P-S,P-S'}$ are equal to 1.40, 2.30, and 0.20 mdyn/Å, respectively, and the bending constants $f_{SPP}$, $f_{SPS}$, and $f_{SPS,SPS}$ are estimated to 1.67, 1.40, and −0.17 mdyn Å/rad, respectively. These results show the predominance of P–S bond strength over P–P interactions as it could be inferred from the vibrational analysis. Moreover the former can be well compared with P–S force constants in $PS_4^{3-}$ (2.53 mdyn/Å) and in $PSO_3^{3-}$ (2.68 mdyn/Å) anions[15] while the latter is considerably weaker than P–P constants in $P_2$ (1.85 mdyn/Å) and in $P_4$ (2.07 mdyn/Å) molecules.[19,20]

For the selenium derivative, the values of the corresponding force constants, $f_{P-P}$ = 1.10 mdyn/Å, $f_{PSe}$ = 1.80 mdyn/Å, $f_{P-Se,P-Se'}$ = 0.20 mdyn/Å, $f_{SePP}$ = 1.65 mdyn Å/rad, $f_{SePSe}$ = 1.37 mdyn Å/rad, and $f_{SePSe,SePSe}$ = −0.18 mdyn Å/rad, lead to similar conclusions. Details about these normal-coordinate calculations will appear elsewhere.[16]

(18) J. H. Schachtschneider in "Vibrational Analysis of Polyatomic Molecules", Parts V and VI, Technical Reports 231-64 and 53-65, Shell Development Co., Emeryville, Calif., 1964 and 1965.
(19) G. R. Somayajulu, *J. Chem. Phys.*, **28**, 814 (1958).
(20) C. W. F. T. Pistorius, *J. Chem. Phys.*, **29**, 1421 (1959).

**Table IV.** Infrared and Raman Band Wavenumbers ($cm^{-1}$) of $MnPS_3$ and $CdPS_3$ Compounds Intercalated with $CrBz_2^+$ in the Solid State at 300 K[a]

| $MnPS_3 \cdot 0.33CrBz_2^+$ | | $CdPS_3 \cdot 0.33CrBz_2^+$ | | approx type of motions |
|---|---|---|---|---|
| IR[b] | R | IR[b] | R | |
| 620 s | 625 w | | | |
| 606 vs | | 606 sh | | |
| 590 sh | 585 w | 595 vs | | $\nu_d(PS_3)$ |
| 570 sh | | 585 sh | | |
| 554 vs | 554 w | 560 s | 560 vw | |
| | | 552 vs | | |
| 464 m | | 464 m | | $tilt_d(CrBz_2^+)$ |
| 449 m | | 451 m | | $T'_z(PS_3)(\nu$(P–P)) |
| 415 s | | 416 s | | $\nu_a(CrBz_2^+)$ |
| 380 w | 384 vs | 375 w | 378 vs | $\nu_s(PS_3)$ |
| | 327 w | | 324 w | $tilt_s(CrBz_2^+)$ |
| 320 m | | 316 m | | $\delta_s(PS_3)$ |
| 297 w | | 300 w | | |
| | 274 s | | 274 s | $\delta_d(PS_3)$ |
| 265 m | 270 sh | | 270 sh | $\nu_s(CrBz_2^+)$ |
| 248 s | 240 w | 248 s | 245 w | $T'_{xy}(PS_3)$ |
| 222 w | 225 w | 231 w<br>225 w | 220 w | $R'_{xy}(PS_3)$ |
| 194 s | | 208 s<br>187 s | | $T'_{xy}(PS_3)$ |
| 148 s | 150 vw | 120 s | 110 w | $R'_{xy}(PS_3) + T'(M)$ |
| | | 97 s | | |
| 110 s | | | | |
| 80 m | | 42 w | | corner Brillouin zone lattice modes |
| 22 s | | | | |

[a] Intensity notations as in Table II. [b] Additional infrared bands assigned to internal modes of Bz rings have been observed: 3068 sh; 3059 m ($\nu$(CH)); 1565 w (1430 + $CrBz_2^+$); 1430 s ($\nu$(C-C); 1145 w, 1001 w ($\delta$(CH)); 970 w ($\nu$(C-C)); 871 w, 792 s ($\gamma$(CH)); 745 w ($tilt_s + \nu_a(CrBz_2^+)$); 716 w ($tilt_d + \nu_s(CrBz_2^+)$); 690 m ($\nu_s + \nu_a(CrBz_2^+)$); 675 sh ($\gamma$(CH), free Bz).

**(d) Temperature Effects on the Vibrational Spectra.** Magnetic measurements performed for $MnPS_3$[21] and $MnPSe_3$[4] over the temperature range from 77 to 300 K have shown susceptibility behavior indicative of antiferromagnetism, with characteristic Neel temperatures equal to 110 and 85 K, respectively. In order to detect any small structural change associated with the magnetic ordering, we recorded Raman spectra of both compounds at low temperatures, down to 10 K. The Raman spectrum of $ZnPS_3$ has been investigated at 10 K for comparison.

No significant changes have been detected on low-temperature spectra of $MnPS_3$. On the other hand, in the spectrum of $MnPSe_3$ weak bands below 150 $cm^{-1}$ are intensified at low temperature, in particular the band at 84 $cm^{-1}$, and weak features at 133–129 $cm^{-1}$ are observed. However, no clear superstructure evidence is found.

For $ZnPS_3$, no large frequency change is observed excluding a low-frequency mode which shifts from 79 to 88 $cm^{-1}$ when the temperature is lowered from 300 to 10 K.

Generally, the half-width of most Raman bands is strongly reduced at 10 K (e.g., the half-width of the band at 259 $cm^{-1}$ for $ZnPS_3$ varies from 10 to 1.5 $cm^{-1}$), and, thus, some small splittings are observed specifically for "degenerate modes" (for instance the 225-$cm^{-1}$ band in $ZnPS_3$ gives two components at 227 and 225 $cm^{-1}$ at 10 K).

Finally, infrared spectra have also been recorded at about 100 K but no significant changes have been observed (Figure 3). However, a weak infrared band at about 530 $cm^{-1}$ always disappears at 100 K; this absorption of second-order nature could be due to a difference combination or to a hot band.

(21) B. E. Taylor, J. Steger, and A. Wold, *J. Solid State Chem.*, **7**, 461 (1973).

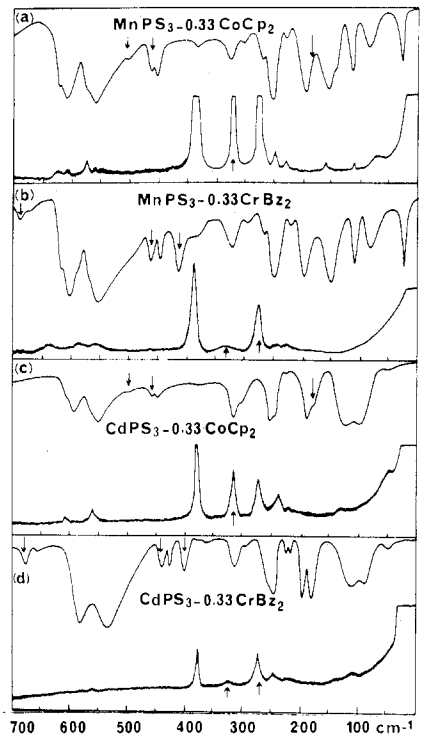


**Figure 4.** Room-temperature infrared and Raman spectra (700–10 $cm^{-1}$) of $CoCp_2^+$ and $CrBz_2^+$ intercalation compounds in $MnPS_3$ and $CdPS_3$. (Arrows indicate bands assigned to internal modes of guest cations, $CoCp_2^+$ and $CrBz_2^+$.)

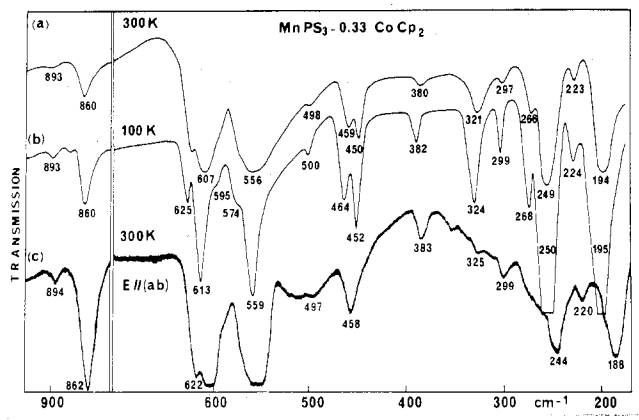


**Figure 5.** Infrared spectra (900–180 $cm^{-1}$) of a polycrystalline sample at 300 K (a) and 100 K (b) and of a platelet at 300 K (c) of the $MnPS_3 \cdot 0.33CoCp_2$ compound.

**2. Intercalated Compounds.** Infrared and Raman spectra (700–10 $cm^{-1}$) of $MnPS_3$ and $CdPS_3$ intercalated with $CoCp_2^+$ and $CrBz_2^+$ are shown in Figure 4. The corresponding band wavenumbers and proposed assignments are reported in Tables III and IV; additional infrared bands observed in the frequency range 4000–700 $cm^{-1}$ and assigned to internal modes of guest species are also listed in these tables. Finally, Figure 5 shows infrared spectra (900–180 $cm^{-1}$) of a polycrystalline sample and of a monocrystalline platelet of $MnPS_3 \cdot 0.33CoCp_2$.

The infrared spectra are essentially a juxtaposition of bands characteristic of the host lattice and of those of the intercalated cations. However, these spectra show a tremendous change for the degenerate $\nu_d(PS_3)$ mode and new weak features (splittings) are observed in the 500–200-$cm^{-1}$ range; we note also new strong low-frequency bands for the manganese derivatives. The Raman spectra of intercalated compounds generally exhibit fewer new features than the infrared ones: the red shift of the visible absorption of these compounds is mainly due to the intrinsic absorption of the guest molecules and is responsible for the poor quality of the Raman spectra.

**(a) Changes of Host Lattice Bands.** First of all, the splitting of the broad 570-$cm^{-1}$ infrared band into two groups of absorptions, at about 600 and 560 $cm^{-1}$, is observed for all the intercalated compounds. This splitting cannot be related to a site distortion larger in intercalated than in unintercalated compounds because the corresponding Raman components (always well resolved) appear at the same frequencies in both kinds of compounds. We have no explanation for the exact meaning of this improvement in the resolution: the weak satellite bands at 625, 595, and 574 $cm^{-1}$ clearly observed at 100 K (Figure 5) could be due to the unit cell multiplicity increase; we have recently obtained a similar experimental result for $In_{2/3}PS_3$.[16] In agreement with this assumption, new weak infrared bands belonging to the modified host lattice spectrum are observed at about 220, 265, 300, and 380 $cm^{-1}$, but the number of these bands is too small to discuss the structural change which has occurred.

However, the main evidence of a different unit cell multiplicity is afforded by the low-frequency strong absorptions observed at 110, 80, and 22 $cm^{-1}$ for manganese derivatives whatever the nature of the intercalated species (Figure 4): these bands can originate from acoustic modes previously in the Brillouin zone boundary for the unintercalated compounds.

**(b) New Bands due to Guest Species.** The presence of guests under the ionic forms $CoCp_2^+$ and $CrBz_2^+$ is easily checked on the frequencies of all the new infrared bands observed in the 3100–700-$cm^{-1}$ region: these bands are characteristic of internal modes of the cations, and the frequencies are very close to those for the corresponding halide salts either in solution or in the solid state.[22] For instance, the bands at 860 and 893 $cm^{-1}$ assigned to $\gamma$(CH) modes of Cp rings would appear for neutral species at 778 and 828 $cm^{-1}$, respectively. Moreover, in the 700–200-$cm^{-1}$ range we observe new bands assigned to metal–ligand tilting and stretching vibrations (Tables III and IV), and frequencies of the antisymmetric modes (infrared bands) are also characteristic of cationic forms.[22] A very strong Raman band at about 320 $cm^{-1}$ is ascribed to the symmetric metal–ring stretching vibrations for $CoCp_2^+$ intercalated compounds. This mode in $CrBz_2^+$ derivatives is smeared under the host lattice band at 274 $cm^{-1}$, but the corresponding tilting mode is clearly seen at about 325 $cm^{-1}$ (Figure 4).

Finally, the broad Raman band observed on the room-temperature spectrum at 68 $cm^{-1}$ for $MnPS_3 \cdot 0.33CoCp_2$ could correspond to an external mode of the cation: when the temperature is lowered to 10 K, this band shifts to 84 $cm^{-1}$ while its half-width changes from $\sim$15 to $\sim$3 $cm^{-1}$. Such a temperature dependence has been observed for low-frequency Raman bands of $FeCp_2$ and $NiCp_2$;[7] in particular, the out-of-plane $R'_{xy}$ libration of Cp rings shifts from 64 $cm^{-1}$ ($\Delta\nu_{1/2}^{300K} \approx 40$ $cm^{-1}$) to 80 $cm^{-1}$ ($\Delta\nu_{1/2}^{10K} \approx 1$ $cm^{-1}$) in nickelocene. By analogy, we conclude that cycles of intercalated $CoCp_2^+$ cations can undergo rotational jumps in the host lattice with a correlation time of the order of $10^{-11}$ s at 300 K. It should be pointed out that temperature-dependent dynamics of cobaltocene molecules intercalated in the layered compound $TaS_2$ have been investigated by proton NMR techniques.[23]

**(c) Orientation of Guest Cations.** Finally, polarized infrared spectra of platelets (Figure 5) show that all the bands due to internal modes of Cp or Bz rings as well as those of metal–ligand vibrations are still intense while the bands at 450 and 320 $cm^{-1}$ assigned to $\nu$(P–P) and $\delta_s(PS_3)$ modes have nearly disappeared. The former group of bands should not be ob-

(22) E. Maslowsky, Jr., in "Vibrational Spectra of Organometallic Compounds", Wiley, New York, 1977, and references therein.
(23) B. G. Silbernagel, *Chem. Phys. Lett.*, **34**, 298 (1975).

served if cycles were lying parallel to (00*l*) layer planes. These observations constitute a first direct experimental result which shows that the highest symmetry axis of guest cations lies parallel to the host lattice layers. A similar assumption has been drawn for the $TaS_2 \cdot 0.25CoCp_2$ compound from a wide-line NMR study.[23]

## Conclusion

This vibrational study was centered around the interpretation of the spectra of the host lattice compounds with respect to their intercalates in order to afford new structural information and to study the dynamics of intercalated molecules.

Results of this study lead to the following conclusions:

Vibrational spectra of unintercalated $MPX_3$ compounds can be interpreted in terms of normal modes of $PX_3$ units weakly bonded through P–P interactions and of translational motions of metal cations.

Spectra of intercalated compounds are, in the first approximation, the superposition of those of the host lattice and of the guest species. This suggests that sandwiches and intercalated "molecules" are weakly interacting.

The guest molecules are intercalated under the cationic forms, $CoCp_2^+$ and $CrBz_2^+$, and from polarized infrared results we conclude that rings are perpendicular to layer planes.

The electron transfer, which occurs during the intercalation of a neutral molecule, does not modify the strength of the P–P interaction. However, the spectra show several perturbations of modes involving P–S bonds.

The main evidence of a different unit cell multiplicity for manganese intercalated compounds is afforded by the observation of new low-frequency intense absorptions.

From low-frequency Raman results, the guest $CoCp_2^+$ ions seem to be dynamically disordered at room temperature and can undergo rotational jumps around their principal axis.

Other layered chalcogenophosphates $MPX_3$, where M = Ni, Fe, ..., are currently under investigation, and the vibrational study of several new intercalates is in progress.

**Acknowledgment.** The authors wish to thank Dr. A. Novak for helpful discussions, Dr. R. Brec and Professor J. Rouxel for a gift of $MnPSe_3$ sample, and Mrs. M. Selim for technical assistance in far-infrared measurements. The authors are also grateful to a reviewer for useful comments.

**Registry No.** $CdPS_3$, 60495-79-6; $ZnPS_3$, 56172-70-4; $MnPS_3$, 59707-74-3; $MnPSe_3$, 69447-58-1; $CoCp_2^+$, 1277-43-6; $CrBz_2^+$, 11077-47-7.

---

Contribution from the Department of Chemistry, The University of Chicago, Chicago, Illinois 60637

# Internal Electron Transfer in Some Four- and Five-Coordinate Macrocyclic Complexes with Copper and Nickel

JEREMY K. BURDETT*[1] and P. DOUGLAS WILLIAMS

*Received December 5, 1979*

Molecular orbital calculations are presented for complexes of difluoro-3,3′-(trimethylenedinitrilo)bis(2-butanone oximato)borate ($LBF_2$) with copper and nickel in I and II oxidation states. In the approximately square-planar complexes $MLBF_2$ with M = $Cu^I$ or $Ni^I$ the $x^2 - y^2$ metal orbital lies above a normally unoccupied ligand $\pi^*$ orbital. This leads to internal electron transfer to the ligand as witnessed experimentally via IR and EPR studies. For M = $Cu^{II}$ or $Ni^{II}$ or for the case where a ligand without conjugated CN groups is used, $x^2 - y^2$ lies below the ligand $\pi^*$ orbitals and such a process does not occur. The presence of a small HOMO–LUMO gap in these species encourages a tetrahedral distortion experimentally observed in the crystal structure of $Cu^ILBF_2$. On CO coordination $x^2 - y^2$ always lies below these $\pi^*$ orbitals. It is found that the CO is attached to the metal largely by interactions between ligand $\sigma$ orbitals and metal 4s and 4p orbitals, augmented by stabilization via unoccupied CO $\pi^*$ orbitals of two metal d orbitals ($\pi$ back-donation). The contribution of the metal d orbitals to the metal–CO $\sigma$ linkage is zero.

## Introduction

There has been recent interest in the study of macrocyclic complexes containing copper atoms as possible models for biochemically important proteins and enzymes. One series of molecules,[2–4] which have been made, contain an apparently $Cu^I$ atom trapped in a distorted square-planar environment (**1**) which readily add carbon monoxide to give the 20-electron species (**2**). There are an interesting series of observations

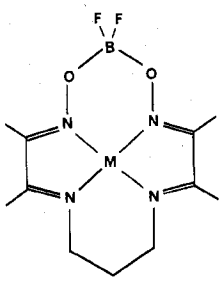


**1**

concerning these complexes which we will rationalize in this paper during the development of their molecular orbital structure.

(i) The free ligand $LBF_2$ has CN stretching vibrations in the region 1600–1650 $cm^{-1}$. In the $MLBF_2$ (**1**) species (M

(1) Fellow of the Alfred P. Sloan Foundation and Henry and Camille Dreyfus Teacher-Scholar.
(2) (a) R. R. Gagné, *J. Am. Chem. Soc.*, **98**, 6709 (1976); (b) R. R. Gagné, J. L. Allison, and G. Lisensky, *Inorg. Chem.*, **17**, 3563 (1978).
(3) R. R. Gagné, J. L. Allison, S. Gall, and C. A. Kovac, *J. Am. Chem. Soc.*, **99**, 7170 (1977).
(4) R. R. Gagné, private communication.

0020-1669/80/1319-2779$01.00/0 